Journal of Visualized Experiments

A method for 3D reconstruction and Virtual Reality analysis of glial and neuronal cells
--Manuscript Draft--

Article Type:	Invited Methods Article - JoVE Produced Video
Manuscript Number:	JoVE59444R2
Full Title:	A method for 3D reconstruction and Virtual Reality analysis of glial and neuronal cells
Keywords:	Glia; astrocytes; Neurons; 3D Reconstruction; Virtual reality; 3D Analysis; VR Analysis; Image segmentation
Corresponding Author:	Corrado Cali', PhD King Abdullah University of Science and Technology Thuwal, Makkakh SAUDI ARABIA
Corresponding Author's Institution:	King Abdullah University of Science and Technology
Corresponding Author E-Mail:	corrado.cali@gmail.com
Order of Authors:	Corrado Cali', PhD
	Kalpana Kare
	Marco Agus
	Maria Fernanda Veloz Castillo
	Daniya Boges
	Markus Hadwiger
	Pierre Magistretti
Additional Information:	
Question	Response
Please indicate whether this article will be Standard Access or Open Access.	Open Access (US$4,200)
Please indicate the **city, state/province, and country** where this article will be **filmed**. Please do not use abbreviations.	Thuwal, Makkah Region, Saudi Arabia

1 **TITLE:**
2 A Method for 3D Reconstruction and Virtual Reality Analysis of Glial and Neuronal Cells
3
4 **AUTHORS & AFFILIATIONS:**
5 Corrado Calì[1], Kalpana Kare[1], Marco Agus[2], Maria Fernanda Veloz Castillo[1], Daniya Boges[1],
6 Markus Hadwiger[2], Pierre Magistretti[1]
7
8 [1]Biological and Environmental Sciences and Engineering Division, King Abdullah University of
9 Science and Technology, Thuwal, Saudi Arabia
10 [2]Visual Computing Center, King Abdullah University of Science and Technology, Thuwal, Saudi
11 Arabia
12
13 Corresponding author:
14 Corrado Calì   (corrado.cali@gmail.com)
15

16 **KEYWORDS:**
17 3DEM, segmentation, 3D reconstruction, 3D analysis, virtual reality, astrocyte
18
19 **SUMMARY:**
20 The described pipeline is designed for the segmentation of electron microscopy datasets larger
21 than gigabytes, to extract whole-cell morphologies. Once the cells are reconstructed in 3D,
22 customized software designed around individual needs can be used to perform a qualitative and
23 quantitative analysis directly in 3D, also using virtual reality to overcome view occlusion.
24
25 **ABSTRACT:**
26 Serial sectioning and subsequent high-resolution imaging of biological tissue using electron
27 microscopy (EM) allow for the segmentation and reconstruction of high-resolution imaged stacks
28 to reveal ultrastructural patterns that could not be resolved using 2D images. Indeed, the latter
29 might lead to a misinterpretation of morphologies, like in the case of mitochondria; the use of
30 3D models is, therefore, more and more common and applied to the formulation of morphology-
31 based functional hypotheses. To date, the use of 3D models generated from light or electron
32 image stacks makes qualitative, visual assessments, as well as quantification, more convenient
33 to be performed directly in 3D. As these models are often extremely complex, a virtual reality
34 environment is also important to be set up to overcome occlusion and to take full advantage of
35 the 3D structure. Here, a step-by-step guide from image segmentation to reconstruction and
36 analysis is described in detail.
37

38 **INTRODUCTION:**
39 The first proposed model for an electron microscopy setup allowing automated serial section and
40 imaging dates back to 1981[1]; the diffusion of such automated, improved setups to image large
41 samples using EM increased in the last ten years[2,3], and works showcasing impressive dense
42 reconstructions or full morphologies immediately followed[4–10].
43
44 The production of large datasets came with the need for improved pipelines for image

45   segmentation. Software tools for the manual segmentation of serial sections, such as
46   RECONSTRUCT and TrakEM2[11,12], were designed for transmission electron microscopy (TEM). As
47   the whole process can be extremely time-consuming, these tools are not appropriate when
48   dealing with the thousands of serial micrographs that can be automatically generated with state-
49   of-the-art, automated EM serial section techniques (3DEM), such as block-face scanning electron
50   microscopy (SBEM)[3] or focused ion beam-scanning electron microscopy (FIB-SEM)[2]. For this
51   reason, scientists put efforts into developing semi-automated tools, as well as fully automated
52   tools, to improve segmentation efficiency. Fully automated tools, based on machine learning[13]
53   or state-of-the-art, untrained pixel classification algorithms[14], are being improved to be used by
54   a larger community; nevertheless, segmentation is still far from being fully reliable, and many
55   works are still based on manual labor, which is inefficient in terms of segmentation time but still
56   provides complete reliability. Semi-automated tools, such as ilastik[15], represent a better
57   compromise, as they provide an immediate readout for the segmentation that can be corrected
58   to some extent, although it does not provide a real proofreading framework, and can be
59   integrated using TrakEM2 in parallel[16].
60
61   Large-scale segmentation is, to date, mostly limited to connectomics; therefore, computer
62   scientists are most interested in providing frameworks for integrated visualizations of large,
63   annotated datasets and analyze connectivity patterns inferred by the presence of synaptic
64   contacts[17,18]. Nevertheless, accurate 3D reconstructions can be used for quantitative
65   morphometric analyses, rather than qualitative assessments of the 3D structures. Tools like
66   NeuroMorph[19,20] and glycogen analysis[10] have been developed to take measurements on the 3D
67   reconstructions for lengths, surface areas, and volumes, and on the distribution of cloud points,
68   completely discarding the original EM stack[8,10]. Astrocytes represent an interesting case study,
69   because the lack of visual clues or repetitive structural patterns give investigators a hint about
70   the function of individual structural units and consequent lack of an adequate ontology of
71   astrocytic processes[21], make it challenging to design analytical tools. One recent attempt was
72   Abstractocyte[22], which allows a visual exploration of astrocytic processes and the inference of
73   qualitative relationships between astrocytic processes and neurites.
74
75   Nevertheless, the convenience of imaging sectioned tissue under EM comes from the fact that
76   the amount of information hidden in intact brain samples is enormous and interpreting single
77   section images can overcome this issue. The density of structures in the brain is so high that 3D
78   reconstructions of even a few objects visible at once would make it impossible to distinguish
79   them visually. For this reason, we recently proposed the use of virtual reality (VR) as an improved
80   method to observe complex structures. We focus on astrocytes[23] to overcome occlusion (which
81   is the blocking of the visibility of an object of interest with a second one, in a 3D space) and ease
82   qualitative assessments of the reconstructions, including proofreading, as well as quantifications
83   of features using count of points in space. We recently combined VR visual exploration with the
84   use of GLAM (glycogen-derived lactate absorption model), a technique to visualize a map of
85   lactate shuttle probability of neurites, by considering glycogen granules as light-emitting
86   bodies[23]; in particular, we used VR to quantify the light peaks produced by GLAM.
87
88   **PROTOCOL:**

1. Image processing using Fiji

1.1. Open the image stack by dragging and dropping the native file from the microscope containing the stack, or by dragging and dropping the folder containing the whole image stack into the software window.

NOTE: Fiji is able to automatically recognize all the standard image formats, such as .jpg, .tif, and .png, as well as proprietary file formats from microscope providers. While the following protocol has been optimized for image stacks from 3DEM, these steps might be used for light microscopy datasets as well.

1.2. Once the stack is opened, go to **Image** > **Properties** to make sure the voxel size has been read from the metadata. If not, it can be manually entered.

1.3. Make sure to transform the image into 8-bit. Click on **Image** > **Type** and select **8-bit**.

1.4. If the original stack was in different sequential files/folders, use **Concatenate** to merge them in a single stack by selecting **Image** > **Stacks** > **Tools** > **Concatenate**.

1.5. Save the stack by selecting **File** > **Save as**. It will be saved as a single .tif file and can be used as a backup and for further processing.

1.6. If the original stack is acquired as different tiles, apply stitching within TrakEM2.

1.6.1. Create a new TrakEM2 project using **New** > **TrakEM2 (blank)**.

1.6.2. Within the viewport graphical user interface (GUI), import the stacks by clicking the right mouse button > **Import** > **Import stack**, and import all the tiles opened in the Fiji main GUI. Make sure to resize the canvas size to fit the entire stack by right-clicking > **Display** > **Resize Canvas/Layer Set**, and choose the *y/x* pixel size depending on the final size of the montage.

NOTE: For instance, if the montage should be finalized using four tiles of 4,096 x 4,096 pixels, the canvas size should be at least 8,192 x 8,192 pixels. Consider make it slightly bigger, and crop it later.

1.6.3. Superimpose the common portions of individual tiles by dragging and dropping them on the layer set. Use the top left slider to modify the transparency to help with the superimposition.

1.6.4. Montage and realign the stacks by clicking the right mouse button > **Align**, and then select one of the options (see note below).

NOTE: SBEM or FIB-SEM are usually already well aligned, but minor misalignments might occur. **Align layers** is the automated pipeline for *z* alignment; **Montage multiple layers** is the automated pipeline for aligning tiles on each *z* stack, for the entire volume; **Align multilayer mosaic** combines

133 the two previous options. This operation is time-consuming and subject to the random-access
134 memory (RAM) of the machine. Consider using a high-end computer and let it run for hours/days,
135 depending on the size of the stack.
136
137 1.6.5. Finally, export the image stacks and save them by using mouse right click > **Make flat**
138 **image**, and then make sure to select the first to the last image in the drop-down menus **Start** and
139 **End**.
140
141 1.6.6. Using TrakEM2 embedded functions, segment structures of interest if needed.
142
143 1.6.6.1. In the TrakEM2's GUI, right-click on **Anything** under the **Template** window and select
144 **Add new child** > **Area_list**.
145
146 1.6.6.2. Drag and drop **Anything** on top of the folder under **Project Objects**, and one **Anything**
147 will appear there.
148
149 1.6.6.3. Drag and drop the **Area list** from the template to the **Anything** located under **Project**
150 **Objects**.
151
152 1.6.6.4. On the image stack viewport, select the **Z space** with the cursor. The area list will appear,
153 with a unique ID number. Select the **brush tool** on top (bottom right) and use the mouse to
154 segment a structure by filling its cytosol, over the whole *z* stack.
155
156 1.6.6.5. Export the segmented mask to be used in ilastik as seed for carving by right-clicking either
157 on the **Area list** object on the Z space list, or on the mask in the viewport, and select **Export** >
158 **Area lists as labels (tif)**.
159
160 1.7. Depending on the resolution needed for further reconstructions, if possible, reduce the pixel
161 size of the image stack by downsampling, considering the memory requirements of the software
162 that will be used for segmentation and reconstruction. Use **Image** > **Adjust** > **Size**.
163
164 NOTE: ilastik handles stacks of up to 500 pixels on *xy* well. Also, downsampling will reduce the
165 resolution of the stack; therefore, take into account the minimum size at which the object still
166 appears recognizable and, thus, can be segmented.
167
168 1.8. To enhance contrast and help the segmentation, the **Unsharp mask** filter can be applied to
169 make membranes crisper. Use **Process** > **Filter** > **Unsharp mask**.
170
171 1.9. Export the image stack as single images for further processing in segmentation software,
172 (e.g., ilastik), using **File** > **Save as...** > **Image sequence** and choose .tif format.
173
174 **2. Segmentation (semi-automated) and reconstruction using ilastik 1.3.2**
175
176 2.1. In the main ilastik GUI, select the **Carving** module.

177

178   2.2. Load the image stack using **Add New** > **Add a single 3D/4D volume from sequence**.

179

180   2.3. Select **Whole directory** and choose the folder containing the image stack saved as single
181   files. At the bottom of the new window, where options for loading the images are present, make
182   sure to keep **Z** selected.

183

184   2.4. For the following steps, all operations and buttons can be found on the left side of the main
185   software GUI. Under the **Preprocessing** tab, use the standard options already checked. Use **bright**
186   **lines (ridge filters)** and keep the filter scale at 1.600. This parameter can be modified afterward.

187

188   2.5. Once the preprocessing is finished, select the next page in the drop-down menu of the
189   **Labeling** module. One **Object** and one **Background** are present by default.

190

191   2.6. Select the object seed by clicking on it, and draw a line on top of the structure of interest;
192   then, select the background seed and draw one or multiple lines outside the object to be
193   reconstructed. Then, click on **Segment**, and wait.

194

195   NOTE: Depending on the power of the computer and the size of the stack, segmentation could
196   take from a few seconds to hours. Once it's done, a semitransparent mask highlighting the
197   segmentation should appear on top of the segmented structure.

198

199   2.6.1. Scroll through the stack to check on the segmentation. The segmentation might not be
200   accurate and not follow the structure of interest accurately or spill out from it. Correct any
201   spillover by placing a background seed on the spilled segmentation, and add an object seed over
202   the nonreconstructed segment of the object of interest.

203

204   2.6.2. If the segmentation is still not correct, try to modify with the **Bias** parameter, which will
205   increase or decrease the amount of uncertain classified pixels as accepted. Its value is 0.95 by
206   default; decrease it to limit any spillover (usually to not less than 0.9) or increase if the
207   segmentation is too conservative (up to 1).

208

209   2.6.3. Another possibility is to go back to step 2.4 (by clicking on **Preprocessing**) and to modify
210   the size of the filter; increasing the value (e.g., to 2) will minimize the salt-and-pepper noise-like
211   effects but will also make membranes more blurred and smaller details harder to detect. This
212   might limit spillover.

213

214   2.7. Reiterate as much as needed, as long as all desired objects have been segmented. Once an
215   object is finished, click on **Save current object**, below **Segment**. Two new seeds will appear, to
216   start the segmentation of a new object.

217

218   2.8. Extract surface meshes right away as .obj files by clicking on **Export all meshes**.

219

220   2.9. If further proofreading is needed, segmentation can be extracted as binary masks. Select the

221 mask to export it by clicking **Browse objects**; then, right-click on **Segmentation** > **Export** and,
222 then, under **Output file info**, select **tif sequence** as format.

223

224 **3. Proofreading/segmentation (manual) in TrakEM2 (Fiji)**

225

226 3.1. Load the image stack and create a new TrekEM2 project as per step 1.6.1.

227

228 3.2. Import the masks that need proofreading using the option **Import labels as arealists**,
229 available in the same import menu used to import the image stack.

230

231 3.3. Select the arealist imported in the Z space and use the **Brush tool** to review the
232 segmentation.

233

234 3.4. Visualize the model in 3D by right-clicking on **Area list** > **Show in 3D**. In the following window
235 asking for a resample number, a higher value will generate a lower resolution mesh.

236

237 NOTE: Depending on the size of the object, consider using a value between 4 and 6, which usually
238 gives the best compromise between resolution and morphological detail.

239

240 3.5. Export the 3D mesh as wavefront .obj by choosing from the menu **File** > **Export surfaces** >
241 **Wavefront**.

242

243 **4. 3D analysis**

244

245 4.1. Open Blender. For the following steps, make sure to install the NeuroMorph toolkit (available
246 at https://neuromorph.epfl.ch/index.html) and the glycogen analysis toolkit (available at
247 https://github.com/daniJb/glyco-analysis).

248

249 4.1.1. Import the objects using the NeuroMorph batch import by clicking **Import Objects** under
250 the **Scene** menu, to import multiple objects at once. Make sure to activate **Use remesh** and
251 **Smooth shading**.

252

253 NOTE: It is not recommended to click on **Finalize remesh** if there is uncertainty about the initial
254 size of the object. **Import tree depth** at value 7 (default) is usually good to maintain an acceptable
255 resolution and morphology of the object.

256

257 4.1.2. Select the object of interest from the outliner and modify the octree depth of the remesh
258 function under the **Modifiers** menu iteratively to minimize the number of vertices and to avoid
259 losing details in resolution and correct morphology. When changing the octree depth, the mesh
260 on the main GUI will change accordingly. Once finished, click on **Apply** to finalize the process.

261

262 NOTE: Values around 4 are usually good for small objects (such as postsynaptic densities), values
263 around 7 for larger ones (such as long axons or dendrites), and values around 8 or 9 for complete
264 cellular morphologies where details of different resolutions should be maintained.

265

266 4.1.3. Use the image superimposition tool **Image stack interactions** on the left panel, under the
267 **NeuroMorph** menu, to load the image stack. Make sure to enter the physical size of the image
268 stack for *x*, *y*, and *x* (in microns or nanometers, depending on the units of the mesh) and select
269 the path of the stack by clicking on **Source_Z**. X and Y are orthogonal planes; they are optional
270 and will be loaded only if the user inserts a valid path.

271

272 4.1.4. Then, select a mesh on the viewport by right-clicking on it, enter the edit mode by pressing
273 **Tab**, select one (or more) vertices using mouse right click, and finally, click on **Show image at**
274 **vertex**. One (or more) cut plane(s) with the micrograph will appear superimposed on top of the
275 mesh.

276

277 4.1.5. Select the cut plane by right-clicking on it, press **Ctrl** + **Y**, and scroll over the 3D model using
278 the mouse scroll. This can also be used as proofreading method.

279

280 4.1.6. Use **Measurement tools** for quantifications of surface areas, volumes, and lengths. These
281 operations are documented in more details by Jorstad et al.[19] and on the NeuroMorph website[24].

282

283 4.1.7. Use the **Glycogen analysis tool** for quantifying glycogen proximity toward spines and
284 boutons. Operations are documented in more details in a previous publication[10] and in the
285 glycogen analysis repository[25].

286

287 4.2. Run GLAM[23]. The code, executable, and some test files are available in the GLAM
288 repository[26].

289

290 4.2.1. Prepare two geometry files in .ply format: one source file containing glycogen granules and
291 one target file containing the morphology surfaces.

292

293 4.2.2. Prepare three .ascii colormap files (each line containing t_norm(0..1) R(0..255) G(0..255)
294 B(0..255)) for representing local absorption values, peak values, and average absorption values.

295

296 4.2.3. Execute the C++ script GLAM, with the geometry files (step 4.2.1) and colormap files (step
297 4.2.2), by setting the influence radius (in microns), the maximum expected absorption value, and
298 a normalized threshold for clustering the absorption peaks. For information about other
299 parameters, execute the script with the –help option.

300

301 4.2.4. Export the results as .ply or .obj files: target objects color-mapped with GLAM values,
302 absorption peak markers represented as color-coded spheres, and target objects color-coded
303 with respect to the mean absorption value.

304

305 4.3. Open VR Data Interact. VR Data Interact-executable code is available in a public repository[27].

306

307 4.3.1. Import meshes to be visualized, following the instructions in the VR menu. Make sure to
308 import the .obj files computed in step 4.2.1, in case a GLAM analysis is needed.

309

REPRESENTATIVE RESULTS:

By using the procedure presented above, we show results on two image stacks of different sizes, to demonstrate how the flexibility of the tools makes it possible to scale up the procedure to larger datasets. In this instance, the two 3DEM datasets are (i) P14 rat, somatosensory cortex, layer VI, 100 μm x 100 μm x 76.4 μm[4] and (ii) P60 rat, hippocampus CA1, 7.07 μm x 6.75 μm x 4.73 μm[10].

The preprocessing steps (**Figure 1**) can be performed the same way for both datasets, simply taking into account that a larger dataset such as the first stack, which is 25 GB, requires more performing hardware to handle large data visualization and processing. The second stack is only 1 GB, with a perfectly isotropic voxel size.

The size of the data might not be directly related to the field of view (FOV), rather than to the resolution of the stack itself, which depends on the maximum pixel size of the sensor of the microscope, and the magnification of the stack. In any case, logically, larger FOVs are likely to occupy more physical space compared to smaller FOVs, if acquired at the same resolution.

Once the image stack is imported, as indicated in section 1 of the protocol, in Fiji software (**Figure 1A**), a scientific release of ImageJ[12], one important point is to make sure that the image format is 8-bit (**Figure 1B**). This because many acquisition software different microscopy companies producers generate their proprietary file format in 16-bit to store metadata relevant to information about the acquiring process (i.e., pixel size, thickness, current/voltage of the electron beam, chamber pressure) together with the image stack. Such adjustments allow scientists to save memory, as the extra 8-bit containing metadata does not affect the images. The second important parameter to check is the voxel size, which then allows the reconstruction following the segmentation to be performed on the correct scale (micrometers or nanometers; **Figure 1B**).

Stacks might need realignment and/or stitching if they have been acquired using tiling; these operations can be performed within TrakEM2 (**Figure 2A**), although regarding realignment, automated 3DEM techniques like FIB-SEM or 3View are usually well realigned.

One last step requires filtering and, possibly, downsampling of the stack, depending on which objects need to be reconstructed and whether downsampling affects the recognition of the reconstructable features. For instance, for the larger stack (of the somatosensory cortex of P14 rats), it was not possible to compromise the resolution for the benefit of the reconstruction efficiency, while for the smaller stack (of the hippocampus CA1 of P60 rats), it was possible to do so because the resolution was far above what was needed for the smallest objects to be reconstructed. Finally, the use of the unsharp mask enhances the difference between the membranes and the background, making it favorable for the reconstructions of software like ilastik which uses gradients to pre-evaluate borders.

Following the image processing, reconstruction can be performed either manually using TrakEM2, or semi-automatically using ilastik (**Figure 2C**). A dataset like the smaller one listed here

353   (ii), that can be downsampled to fit into memory, can be fully segmented using ilastik (**Figure 2B**)
354   to produce a dense reconstruction. In the case of the first dataset listed here (i), we have
355   managed to load and preprocess the entire dataset with a Linux workstation with 500 GB of RAM.
356   The sparse segmentation of 16 full morphologies was obtained with a hybrid pipeline, by
357   extracting rough segmentation that was manually proofread using TrakEM2.

359   The 3D analysis of features like surface areas, volumes, or the distribution of intracellular
360   glycogen can be performed within a Blender environment (**Figure 3**) using custom codes, such as
361   NeuroMorph[19] or glycogen analysis[10].

363   In case of datasets containing glycogen granules as well, analysis on their distribution can be
364   inferred using GLAM, a C++ code that would generate colormaps with influence area directly on
365   the mesh.

367   Finally, such complex datasets can be visualized and analyzed using VR, which has been proven
368   to be useful for the analysis of datasets with a particular occluded view (**Figure 4**). For instance,
369   peaks inferred from GLAM maps were readily inferred visually from dendrites in the second
370   dataset discussed here.

372   **FIGURE AND TABLE LEGENDS:**

374   **Figure 1: Image processing and preparation for image segmentation**. (**a**) Main Fiji GUI. (**b**)
375   Example of stacked images from dataset (i) discussed in the representative results. The panel on
376   the right shows properties allowing the user to set the voxel size. (**c**) Example of a filer and resize
377   operation applied to a single image. The panels on the right show magnifications from the center
378   of the image.

380   **Figure 2: Segmentation and reconstruction using TrakEM2 and ilastik.** (**a**) TrakEM2 GUI with
381   objects manually segmented (in red). (**b**) The exported mask from panel **a** can be used as input
382   (seed) for (**c**) semi-automated segmentation (carving). From ilastik, masks (red) can be further
383   exported to TrakEM2 for manual proofreading. (**d**) Masks can be then exported as 3D triangular
384   meshes to reveal reconstructed structures. In this example, four neurons, astrocytes, microglia,
385   and pericytes from dataset (i) (discussed in the representative results) were reconstructed using
386   this process.

388   **Figure 3: 3D analysis of reconstructed morphologies using customized tools.** (**a**) Isotropic
389   imaged volume from FIB-SEM dataset (ii) (as discussed in the representative results). (**b**) Dense
390   reconstruction from panel **a**. Grey = axons; green = astrocytic process; blue = dendrites. (**c**)
391   Micrograph showing examples of targets for quantifications such as synapses (dataset (i)) and
392   astrocytic glycogen granules (dataset (ii)) in the right magnifications. (**d**) Mask from panel **c**
393   showing the distribution of glycogen granules around synapses. (**e**) Quantification of glycogen
394   distribution from the dataset from panel **c**, using the glycogen analysis toolbox from Blender. The
395   error bars indicate standard errors. N = 4,145 glycogen granules. (**f**) A graphic illustration of the
396   input and output visualization of GLAM.

397
Figure 4: Analysis in VR. (**a**) A user wearing a VR headset while working on (**b**) the dense reconstruction from FIB-SEM dataset (ii) (as discussed in the representative results). (**c**) Immersive VR scene from a subset of neurites from panel **b**. The green laser is pointing to a GLAM peak. (**d**) Example of an analysis from GLAM peak counts in VR. $N = 3$ mice per each bar. Analysis of FIB-SEM from a previous publication[28]. The error bars indicate the standard errors; *$p < 0.1$, one-way ANOVA.

DISCUSSION:
The method presented here is a useful step-by-step guide for the segmentation and 3D reconstruction of a multiscale EM dataset, whether they come from high-resolution imaging techniques, like FIB-SEM, or other automated serial sectioning and imaging techniques. FIB-SEM has the advantage of potentially reaching perfect isotropy in voxel size by cutting sections as thin as 5 nm using a focused ion beam, its FOV might be limited to 15–20 µm because of side artifacts, which are possibly due to the deposition of the cut tissue if the FOV exceeds this value. Such artifacts can be avoided by using other techniques, such as SBEM, which uses a diamond knife to cut serial sections inside the microscope chamber. In this latter case, the *z* resolution can be around 20 nm at best (usually, 50 nm), but the FOV might be larger, although the pixel resolution should be compromised for a vast region of interest. One solution to overcome such limitations (magnification vs. FOV) is to divide the region of interest in tiles and acquire each of them at a higher resolution. We have shown here results from both an SBEM stack—dataset (i) in the representative results—and a FIB-SEM stack—dataset (ii) in the representative results.

As the generation of larger and larger datasets is becoming increasingly more common, efforts in creating tools for pixel classification and automated image segmentation are multiplying; nevertheless, to date, no software has proven reliability comparable to that of human proofreading, which is therefore still necessary, no matter how time-consuming it is. In general, smaller datasets that can be downsampled, like in the case of dataset (ii), can be densely reconstructed by a single, expert user in a week, including proofreading time.

The protocol presented here involves the use of three software programs in particular: Fiji (version 2.0.0-rc-65/1.65b), ilastik (version 1.3.2 rc2), and Blender (2.79), which are all open-source and multi-platform programs and downloadable for free. Fiji is a release of ImageJ, powered by plugins for biological image analysis. It has a robust software architecture and is suggested as it is a common platform for life scientists and includes TrakEM2, one of the first and most widely used plugins for image segmentation. One issue experienced by many users lately is the transition from Java 6 to Java 8, which is creating compatibility issues; therefore, we suggest refraining from updating to Java 8, if possible, to allow Fiji to work properly. ilastik is a powerful software providing a number of frameworks for pixel classification, each one documented and explained on their website. The carving module used for the semi-automated segmentation of EM stacks is convenient as it saves much time, allowing scientists to reduce the time spent on manual work from months to days for an experienced user, as with a single click an entire neurite can be segmented in seconds. The preprocessing step is very intense from a hardware point of view, and very large datasets, like the SBEM stack presented here, which was 26 GB, require

peculiar strategies to fit into memory, considering that one would acquire large dataset because cannot compromise field of view and resolution. Therefore, downsampling might not be an appropriate solution in this case. The latest release of the software can do the preprocessing in a few hours with a powerful Linux workstation, but the segmentation would take minutes, and scrolling through the stack would still be relatively slow. We still use this method for a first, rough segmentation, and proofread it using TrakEM2. Finally, Blender is a 3D modeling software, with a powerful 3D rendering engine, which can be customized with python scripts that can be embedded in the main GUI as add-ons, such as NeuroMorph and glycogen analysis. The flexibility of this software comes with the drawback that, in contrast to Fiji, for instance, it is not designed for the online visualization of large datasets; therefore, visualizing and navigating through large meshes (exceeding 1 GB) might be slow and not efficient. Because of this, it is always advisable to choose techniques that reduce mesh complexity but are careful not to disrupt the original morphology of the structure of interest. The remesh function comes in handy and is an embedded feature of the NeuroMorph batch import tool. An issue with this function is that, depending on the number of vertices of the original mesh, the octree depth value, which is related to the final resolution, should be modified accordingly. Small objects can be remeshed with a small octree depth (e.g., 4), but the same value might disrupt the morphology of larger objects, which needs bigger values (6 at best, to 8 or even 9 for a very big mesh, such as a full cell). It is advisable to make this process iterative and test the different octree depths if the size of the object is not clear.

As mentioned previously, one aspect that should be taken into account is the computational power to be dedicated to reconstruction and analysis, related to the software that is being used. All the operations shown in the representative results of this manuscript were obtained using a MacPro, equipped with an AMD FirePro D500 Graphics card, 64 GB of RAM, and an Intel Xeon E5 CPU with 8 cores. Fiji has a good software architecture for handling large datasets; therefore, it is recommended to use a laptop with a good hardware performance, such as a MacBook Pro with a 2.5 GHz Intel i7 CPU and 16 GB of RAM. ilastik software is more demanding in terms of hardware resources, in particular during the preprocessing step. Although downsampling the image stack is a good trick to limit the hardware requests from the software and allows the user to process a stack with a laptop (typically if it is below 500 pixels in *x,y,z*), we suggest the use of a high-end computer to run this software smoothly. We use a workstation equipped with an Intel Xeon Gold 6150 CPU with 16 cores and 500 GB of RAM.

When provided with an accurate 3D reconstruction, scientists can discard the original micrographs and work directly on the 3D models to extract useful morphometric data to compare cells of the same type, as well as different types of cells, and take advantage of VR for qualitative and quantitative assessments of the morphologies. In particular, the use of the latter has proven to be beneficial in the case of analyses of dense or complex morphologies that present visual occlusion (i.e., the blockage of view of an object of interest in the 3D space by a second one placed between the observer and the first object), making it difficult to represent and analyze them in 3D. In the example presented, an experienced user took about 4 nonconsecutive hours to observe the datasets and count the objects. The time spent on VR analysis might vary as aspects like VR sickness (which can, to some extent, be related to car sickness) can have a

485 negative impact on the user experience; in this case, the user might prefer other analysis tools
486 and limit their time dedicated to VR.
487
488 Finally, all these steps can be applied to other microscopy and non-EM techniques that generate
489 image stacks. EM generates images that are, in general, challenging to handle and segment,
490 compared with, for instance, fluorescence microscopy, where something comparable to a binary
491 mask (signal versus a black background), that in principle can be readily rendered in 3D for further
492 processing, often needs to be dealt with.
493

498
499 **DISCLOSURES:**
500 The authors have nothing to disclose.
501

502 **REFERENCES:**
503 1. Leighton, S. B. SEM images of block faces, cut by a miniature microtome within the SEM - a
504 technical note. *Scanning Electron Microscopy.* 73–76 (1981).
505 2. Knott, G., Marchman, H., Wall, D., Lich, B. Serial section scanning electron microscopy of adult
506 brain tissue using focused ion beam milling. *Journal of Neuroscience.* **28**, 2959–2964 (2008).
507 3. Denk, W., Horstmann, H. Serial block-face scanning electron microscopy to reconstruct three-
508 dimensional tissue nanostructure. *PLOS Biology.* **2**, e329 (2004).
509 4. Coggan, J. S. et al. A Process for Digitizing and Simulating Biologically Realistic Oligocellular
510 Networks Demonstrated for the Neuro-Glio-Vascular Ensemble. *Frontiers in Neuroscience.* **12**
511 (2018).
512 5. Tomassy, G. S. et al. Distinct Profiles of Myelin Distribution Along Single Axons of Pyramidal
513 Neurons in the Neocortex. *Science.* **344**, 319–324 (2014).
514 6. Wanner, A. A., Genoud, C., Masudi, T., Siksou, L., Friedrich, R. W. Dense EM-based
515 reconstruction of the interglomerular projectome in the zebrafish olfactory bulb. *Nature
516 Neuroscience.* **19**, 816–825 (2016).
517 7. Kasthuri, N. et al. Saturated Reconstruction of a Volume of Neocortex. *Cell.* **162**, 648–661
518 (2015).
519 8. Calì, C. et al. The effects of aging on neuropil structure in mouse somatosensory cortex—A 3D
520 electron microscopy analysis of layer 1. *PLOS ONE.* **13**, e0198131 (2018).
521 9. Calì, C., Agus, M., Gagnon, N., Hadwiger, M., Magistretti, P. J. Visual Analysis of Glycogen
522 Derived Lactate Absorption in Dense and Sparse Surface Reconstructions of Rodent Brain
523 Structures. *Eurographics Italian Chapter Conference 2017 – Smart Tools and Apps in computer
524 Graphics*. Catania, Italy (2017).
525 10. Calì, C. et al. Three-dimensional immersive virtual reality for studying cellular compartments
526 in 3D models from EM preparations of neural tissues. *Journal of Comparative Neurology.* **524**,
527 23–38 (2016).
528 11. Fiala, J. C. Reconstruct: a free editor for serial section microscopy. *Journal of Microscopy.* **218**,

52–61 (2005).

12. Cardona, A. et al. TrakEM2 software for neural circuit reconstruction. *PLOS ONE.* **7**, e38011 (2012).

13. Januszewski, M. et al. High-precision automated reconstruction of neurons with flood-filling networks. *Nature Methods.* **1** (2018).

14. Shahbazi, A. et al. Flexible Learning-Free Segmentation and Reconstruction of Neural Volumes. *Scientific Reports.* **8**, 14247 (2018).

15. Sommer, C., Straehle, C., Köthe, U., Hamprecht, F. A. Ilastik: Interactive learning and segmentation toolkit. *2011 IEEE International Symposium on Biomedical Imaging: From Nano to Macro.* Chicago, IL (2011).

16. Holst, G., Berg, S., Kare, K., Magistretti, P., Calì, C. Adding large EM stack support. *2016 4th Saudi International Conference on Information Technology (Big Data Analysis) (KACSTIT).* Riyadh, Saudi Arabia (2016).

17. Beyer, J. et al. ConnectomeExplorer: query-guided visual analysis of large volumetric neuroscience data. *IEEE Transactions on Visualization and Computer Graphics.* **19**, 2868–2877 (2013).

18. Beyer, J. et al. Culling for Extreme-Scale Segmentation Volumes: A Hybrid Deterministic and Probabilistic Approach. *IEEE Transactions on Visualization and Computer Graphics.* doi:10.1109/TVCG.2018.2864847 (2018).

19. Jorstad, A. *et al.* NeuroMorph: A Toolset for the Morphometric Analysis and Visualization of 3D Models Derived from Electron Microscopy Image Stacks. *Neuroinformatics.* **13**, 83–92 (2015).

20. Jorstad, A., Blanc, J., Knott, G. NeuroMorph: A Software Toolset for 3D Analysis of Neurite Morphology and Connectivity. *Frontiers in Neuroanatomy.* **12**, 59 (2018).

21. Calì, C. Astroglial anatomy in the times of connectomics. *Journal of Translational Neuroscience.* **2**, 31–40 (2017).

22. Mohammed, H. et al. Abstractocyte: A Visual Tool for Exploring Nanoscale Astroglial Cells. *IEEE Transactions on Visualization and Computer Graphics.* doi:10.1109/TVCG.2017.2744278 (2017).

23. Agus, M. et al. GLAM: Glycogen-derived Lactate Absorption Map for visual analysis of dense and sparse surface reconstructions of rodent brain structures on desktop systems and virtual environments. *Computers & Graphics.* **74**, 85–98 (2018).
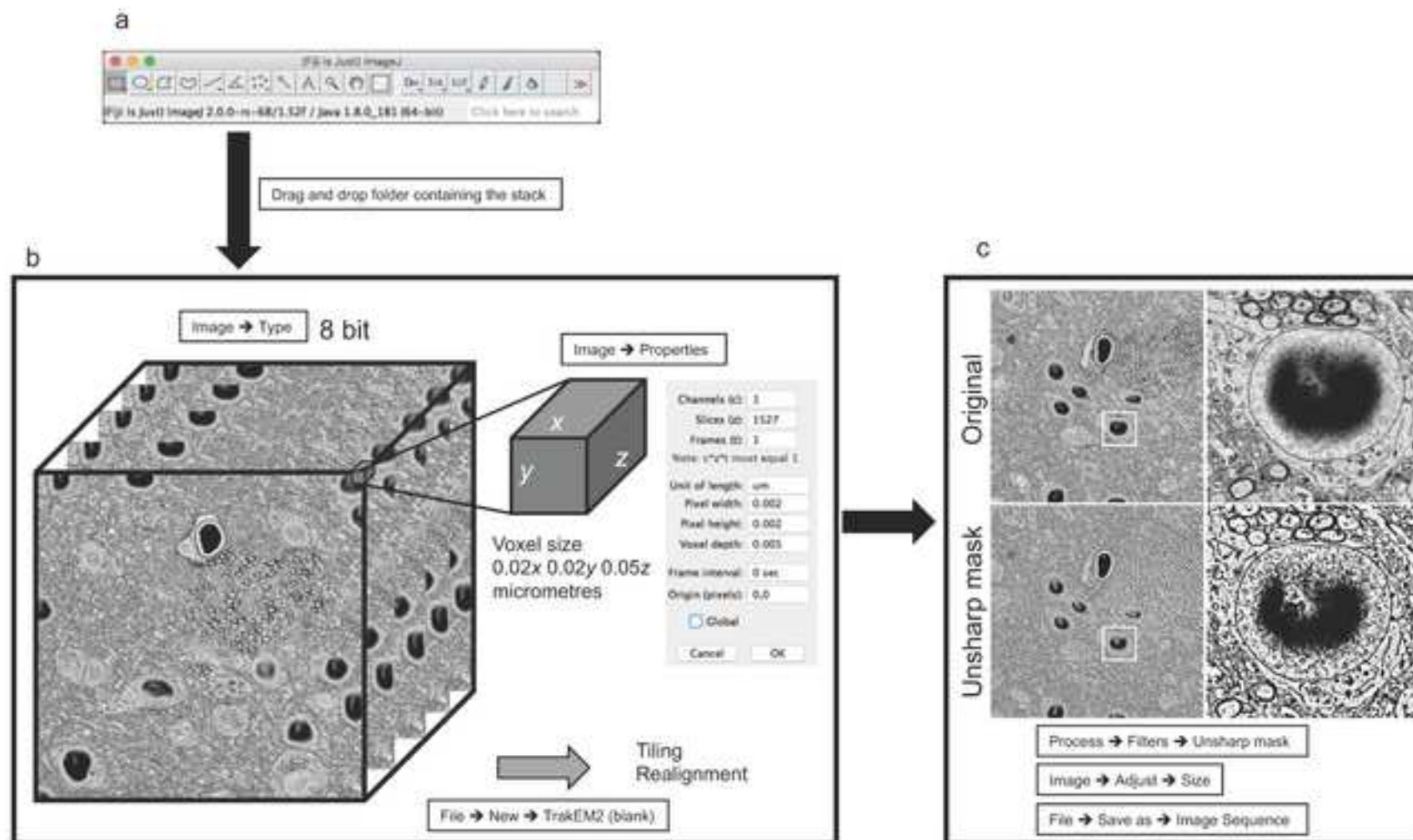
24. École Polytechnique Fédérale de Lausanne. NeuroMorph Analysis and Visualization Toolset. http://neuromorph.epfl.ch/ (2018).

25. Boges, D. GitHub - daniJb/glycol-analysis: Glycogen_analysis.py is a python-blender API based script that performs analysis on a reconstructed module of glycogen data. https://github.com/daniJb/glyco-analysis (2018).

26. Agus, M. GitHub – magus74/GLAM: Glycogen Lactate Absorption Model. https://github.com/magus74/GLAM (2019).

27. Agus, M. et al. GLAM: Glycogen-derived Lactate Absorption Map for visual analysis of dense and sparse surface reconstructions of rodent brain structures on desktop systems and virtual environments. *Dryad Digital Repository.* 10.5061/dryad.808k4r0 (2018).

28. Calì, C. et al. Data from: The effects of aging on neuropil structure in mouse somatosensory cortex—A 3D electron microscopy analysis of layer 1. *Dryad Digital Repository.* doi:10.5061/dryad.bh78sn5 (2018).

Figure 1
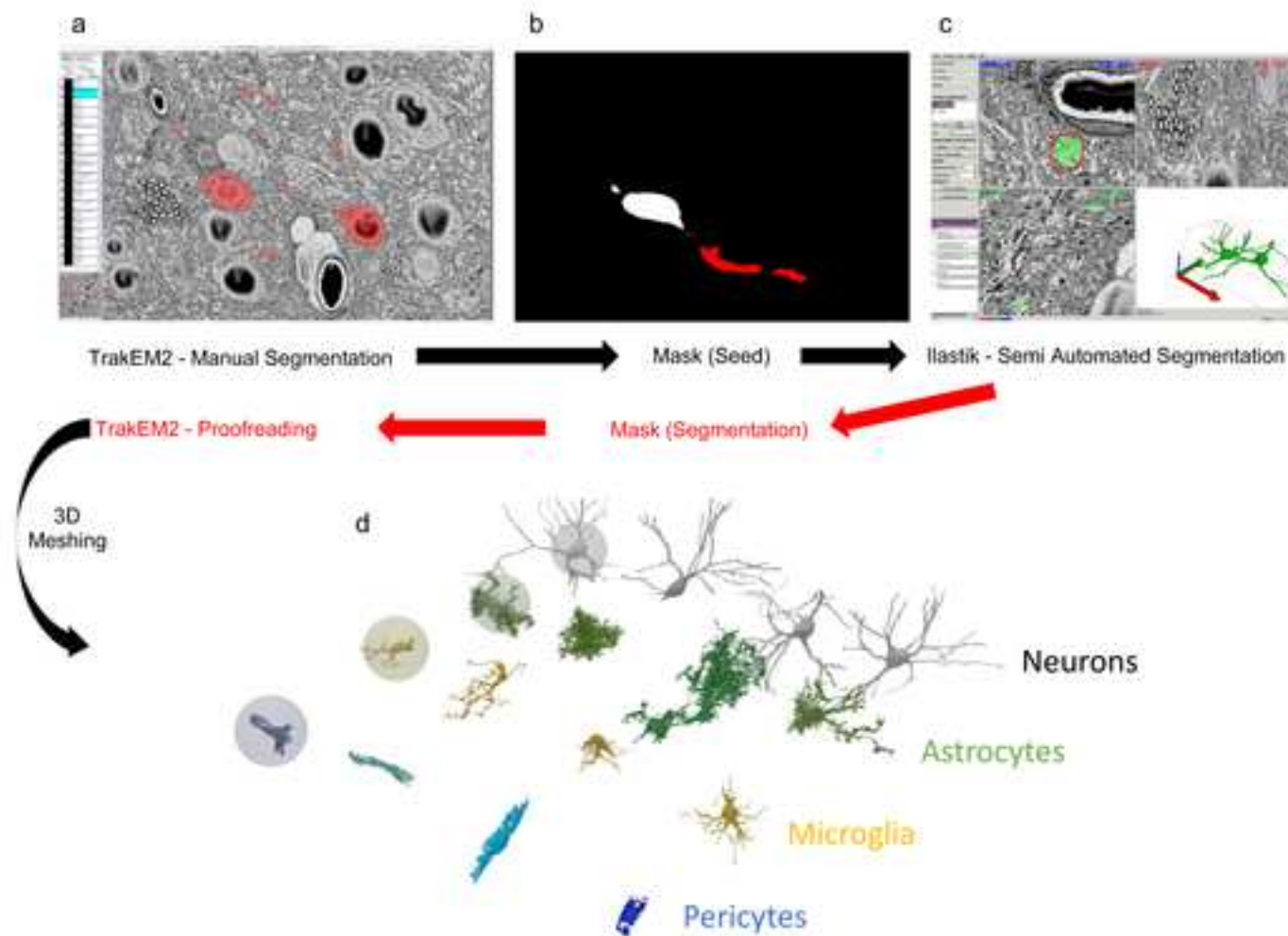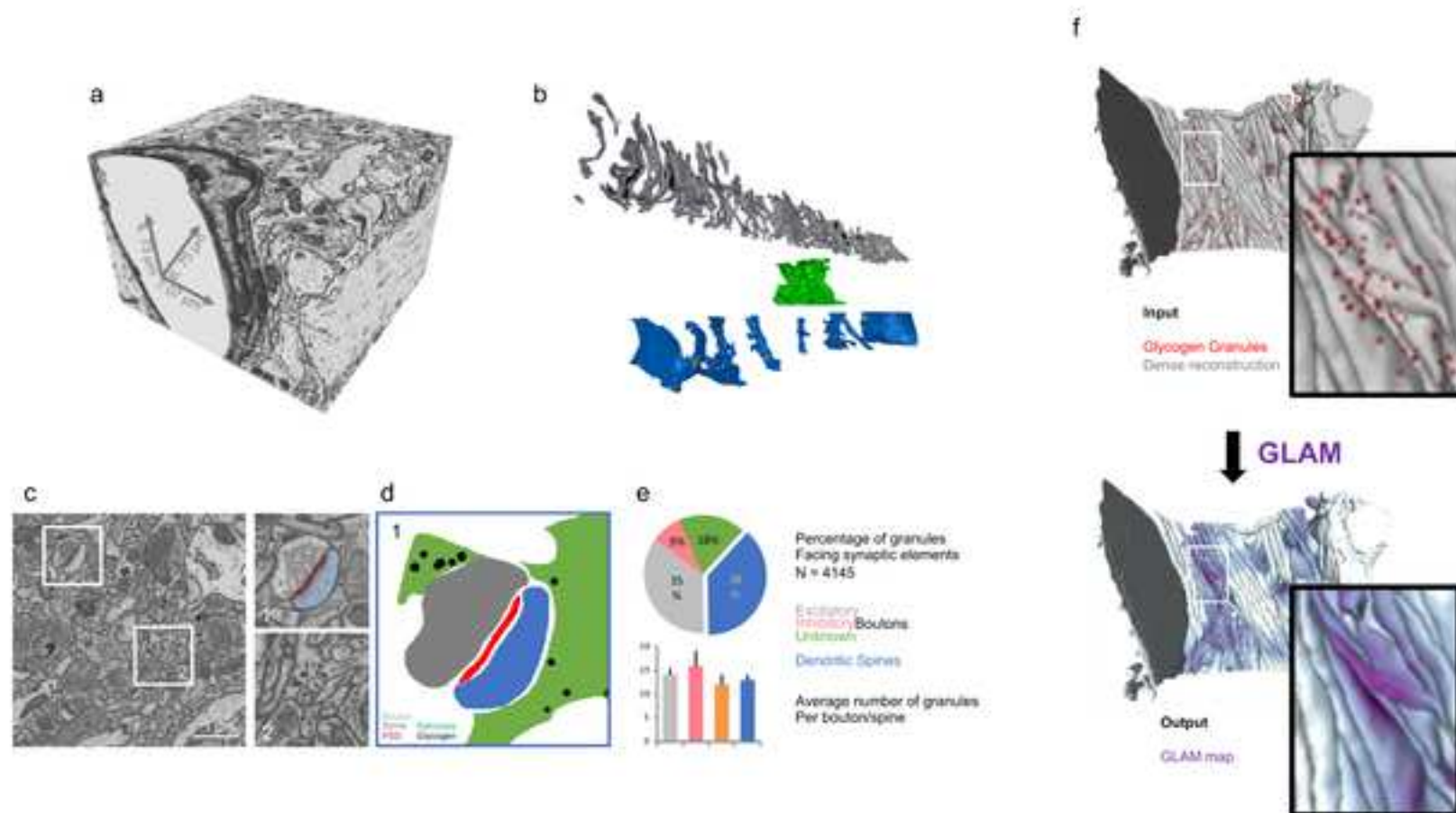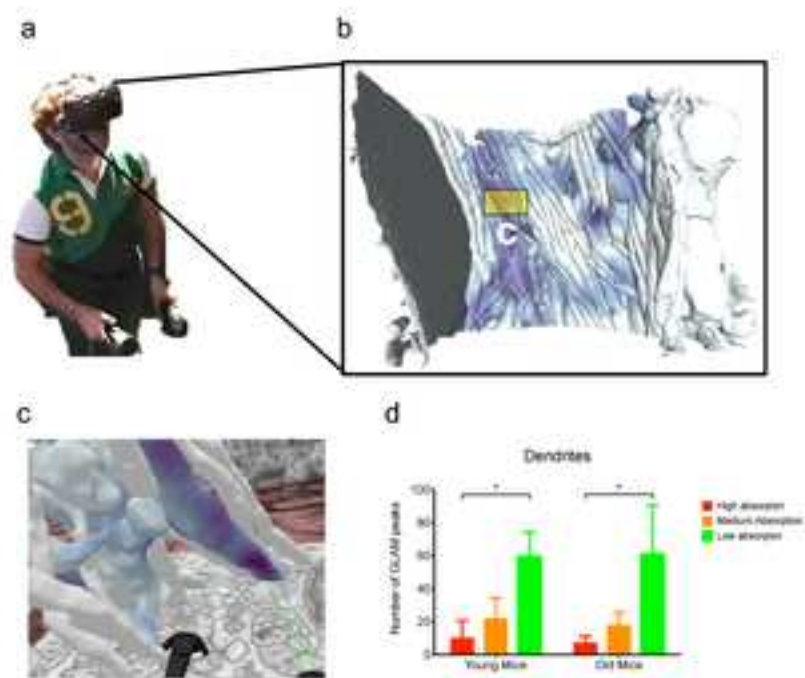
Figure 1

Figure 2

Click here to access/download;Figure;Figure 2.tiff ±

a

b

c

TrakEM2 - Manual Segmentation → Mask (Seed) → Ilastik - Semi Automated Segmentation

TrakEM2 - Proofreading ← Mask (Segmentation) ←

3D Meshing

d

Neurons

Astrocytes

Microglia

Pericytes

Figure 3

a

b

c

d

1

e

Percentage of granules
Facing synaptic elements
N = 4145

Excitatory
Inhibitory Boutons
Unknown

Dendritic Spines

Average number of granules
Per bouton/spine

2

Bouton
Spine   Extrusions
PSD   Glycogen

f

Input

Glycogen Granules
Dense reconstruction

GLAM

Output

GLAM map

Figure 4

Click here to access/download;Figure;Figure 4.tiff ⬇

Name of Material/ Equipment	Company	Catalog Number/Version	Comments/Description
Fiji	Open Source	2.0.0-rc-65/1.65b	Open Source image processing editor
iLastik	Open Source	1.3.2 rc2	Image Segmentation tool
Blender	Blender Foundation	2.79	Open Source 3D Modeling software
HTC Vive Headset	HTC	Vive / Vive Pro	Virtual Reality (VR) Head monted headset
Neuromorph	Open Source	---	Collection of Blender Addons for 3D Analysi
Glycogen Analysis	Open Source	---	Blender addon for analysis of Glycogen
GLAM	Open Source	---	C++ Code For generating GLAM Maps

Website

www.fiji.sc
www.ilastik.org
www.blender.org
www.vive.com
neuromorph.epfl.ch
https://github.com/daniJb/glyco-analysis
https://github.com/magus74/GLAM

jove
JOURNAL OF
VISUALIZED EXPERIMENTS

1 Alewife Center #200
Cambridge, MA 02140
tel. 617.945.9051
www.jove.com

ARTICLE AND VIDEO LICENSE AGREEMENT

Title of Article:

> A method for 3D reconstruction and Virtual Reality analysis of glial and neuronal cells

Author(s):

> Corrado Cali, Kalpana Kare, Marco Agus, Daniya Boges, Markus Hadwiger, Pierre J. Magistretti

Item 1: The Author elects to have the Materials be made available (as described at http://www.jove.com/publish) via:

☐ Standard Access   ☑ Open Access

Item 2: Please select one of the following items:

☑ The Author is **NOT** a United States government employee.

☐ The Author is a United States government employee and the Materials were prepared in the course of his or her duties as a United States government employee.

☐ The Author is a United States government employee but the Materials were NOT prepared in the course of his or her duties as a United States government employee.

ARTICLE AND VIDEO LICENSE AGREEMENT

1.   **Defined Terms.** As used in this Article and Video License Agreement, the following terms shall have the following meanings: "**Agreement**" means this Article and Video License Agreement; "**Article**" means the article specified on the last page of this Agreement, including any associated materials such as texts, figures, tables, artwork, abstracts, or summaries contained therein; "**Author**" means the author who is a signatory to this Agreement; "**Collective Work**" means a work, such as a periodical issue, anthology or encyclopedia, in which the Materials in their entirety in unmodified form, along with a number of other contributions, constituting separate and independent works in themselves, are assembled into a collective whole; "**CRC License**" means the Creative Commons Attribution-Non Commercial-No Derivs 3.0 Unported Agreement, the terms and conditions of which can be found at: http://creativecommons.org/licenses/by-nc-nd/3.0/legalcode; "**Derivative Work**" means a work based upon the Materials or upon the Materials and other pre-existing works, such as a translation, musical arrangement, dramatization, fictionalization, motion picture version, sound recording, art reproduction, abridgment, condensation, or any other form in which the Materials may be recast, transformed, or adapted; "**Institution**" means the institution, listed on the last page of this Agreement, by which the Author was employed at the time of the creation of the Materials; "**JoVE**" means MyJove Corporation, a Massachusetts corporation and the publisher of The Journal of Visualized Experiments; "**Materials**" means the Article and / or the Video; "**Parties**" means the Author and JoVE; "**Video**" means any video(s) made by the Author, alone or in conjunction with any other parties, or by JoVE or its affiliates or agents, individually or in collaboration with the Author or any other parties, incorporating all or any portion of the Article, and in which the Author may or may not appear.

2.   **Background.** The Author, who is the author of the Article, in order to ensure the dissemination and protection of the Article, desires to have the JoVE publish the Article and create and transmit videos based on the Article. In furtherance of such goals, the Parties desire to memorialize in this Agreement the respective rights of each Party in and to the Article and the Video.

3.   **Grant of Rights in Article.** In consideration of JoVE agreeing to publish the Article, the Author hereby grants to JoVE, subject to **Sections 4** and **7** below, the exclusive, royalty-free, perpetual (for the full term of copyright in the Article, including any extensions thereto) license (a) to publish, reproduce, distribute, display and store the Article in all forms, formats and media whether now known or hereafter developed (including without limitation in print, digital and electronic form) throughout the world, (b) to translate the Article into other languages, create adaptations, summaries or extracts of the Article or other Derivative Works (including, without limitation, the Video) or Collective Works based on all or any portion of the Article and exercise all of the rights set forth in (a) above in such translations, adaptations, summaries, extracts, Derivative Works or Collective Works and (c) to license others to do any or all of the above. The foregoing rights may be exercised in all media and formats, whether now known or hereafter devised, and include the right to make such modifications as are technically necessary to exercise the rights in other media and formats. If the "Open Access" box has been checked in **Item 1** above, JoVE and the Author hereby grant to the public all such rights in the Article as provided in, but subject to all limitations and requirements set forth in, the CRC License.

612542.6   For questions, please contact us at submissions@jove.com or +1.617.945.9051.

4.   **Retention of Rights in Article.** Notwithstanding the exclusive license granted to JoVE in **Section 3** above, the Author shall, with respect to the Article, retain the non-exclusive right to use all or part of the Article for the non-commercial purpose of giving lectures, presentations or teaching classes, and to post a copy of the Article on the Institution's website or the Author's personal website, in each case provided that a link to the Article on the JoVE website is provided and notice of JoVE's copyright in the Article is included. All non-copyright intellectual property rights in and to the Article, such as patent rights, shall remain with the Author.

5.   **Grant of Rights in Video – Standard Access.** This **Section 5** applies if the "Standard Access" box has been checked in **Item 1** above or if no box has been checked in **Item 1** above. In consideration of JoVE agreeing to produce, display or otherwise assist with the Video, the Author hereby acknowledges and agrees that, Subject to **Section 7** below, JoVE is and shall be the sole and exclusive owner of all rights of any nature, including, without limitation, all copyrights, in and to the Video. To the extent that, by law, the Author is deemed, now or at any time in the future, to have any rights of any nature in or to the Video, the Author hereby disclaims all such rights and transfers all such rights to JoVE.

6.   **Grant of Rights in Video – Open Access.** This **Section 6** applies only if the "Open Access" box has been checked in **Item 1** above. In consideration of JoVE agreeing to produce, display or otherwise assist with the Video, the Author hereby grants to JoVE, subject to **Section 7** below, the exclusive, royalty-free, perpetual (for the full term of copyright in the Article, including any extensions thereto) license (a) to publish, reproduce, distribute, display and store the Video in all forms, formats and media whether now known or hereafter developed (including without limitation in print, digital and electronic form) throughout the world, (b) to translate the Video into other languages, create adaptations, summaries or extracts of the Video or other Derivative Works or Collective Works based on all or any portion of the Video and exercise all of the rights set forth in (a) above in such translations, adaptations, summaries, extracts, Derivative Works or Collective Works and (c) to license others to do any or all of the above. The foregoing rights may be exercised in all media and formats, whether now known or hereafter devised, and include the right to make such modifications as are technically necessary to exercise the rights in other media and formats. For any Video to which this **Section 6** is applicable, JoVE and the Author hereby grant to the public all such rights in the Video as provided in, but subject to all limitations and requirements set forth in, the CRC License.

7.   **Government Employees.** If the Author is a United States government employee and the Article was prepared in the course of his or her duties as a United States government employee, as indicated in **Item 2** above, and any of the licenses or grants granted by the Author hereunder exceed the scope of the 17 U.S.C. 403, then the rights granted hereunder shall be limited to the maximum

rights permitted under such statute. In such case, all provisions contained herein that are not in conflict with such statute shall remain in full force and effect, and all provisions contained herein that do so conflict shall be deemed to be amended so as to provide to JoVE the maximum rights permissible within such statute.

8.   **Protection of the Work.** The Author(s) authorize JoVE to take steps in the Author(s) name and on their behalf if JoVE believes some third party could be infringing or might infringe the copyright of either the Author's Article and/or Video.

9.   **Likeness, Privacy, Personality.** The Author hereby grants JoVE the right to use the Author's name, voice, likeness, picture, photograph, image, biography and performance in any way, commercial or otherwise, in connection with the Materials and the sale, promotion and distribution thereof. The Author hereby waives any and all rights he or she may have, relating to his or her appearance in the Video or otherwise relating to the Materials, under all applicable privacy, likeness, personality or similar laws.

10.   **Author Warranties.** The Author represents and warrants that the Article is original, that it has not been published, that the copyright interest is owned by the Author (or, if more than one author is listed at the beginning of this Agreement, by such authors collectively) and has not been assigned, licensed, or otherwise transferred to any other party. The Author represents and warrants that the author(s) listed at the top of this Agreement are the only authors of the Materials. If more than one author is listed at the top of this Agreement and if any such author has not entered into a separate Article and Video License Agreement with JoVE relating to the Materials, the Author represents and warrants that the Author has been authorized by each of the other such authors to execute this Agreement on his or her behalf and to bind him or her with respect to the terms of this Agreement as if each of them had been a party hereto as an Author. The Author warrants that the use, reproduction, distribution, public or private performance or display, and/or modification of all or any portion of the Materials does not and will not violate, infringe and/or misappropriate the patent, trademark, intellectual property or other rights of any third party. The Author represents and warrants that it has and will continue to comply with all government, institutional and other regulations, including, without limitation all institutional, laboratory, hospital, ethical, human and animal treatment, privacy, and all other rules, regulations, laws, procedures or guidelines, applicable to the Materials, and that all research involving human and animal subjects has been approved by the Author's relevant institutional review board.

11.   **JoVE Discretion.** If the Author requests the assistance of JoVE in producing the Video in the Author's facility, the Author shall ensure that the presence of JoVE employees, agents or independent contractors is in accordance with the relevant regulations of the Author's institution. If more than one author is listed at the beginning of this Agreement, JoVE may, in its sole

![JoVE logo - JOURNAL OF VISUALIZED EXPERIMENTS]

1 Alewife Center #200
Cambridge, MA 02140
tel. 617.945.9051
www.jove.com

ARTICLE AND VIDEO LICENSE AGREEMENT

discretion, elect not take any action with respect to the Article until such time as it has received complete, executed Article and Video License Agreements from each such author. JoVE reserves the right, in its absolute and sole discretion and without giving any reason therefore, to accept or decline any work submitted to JoVE. JoVE and its employees, agents and independent contractors shall have full, unfettered access to the facilities of the Author or of the Author's institution as necessary to make the Video, whether actually published or not. JoVE has sole discretion as to the method of making and publishing the Materials, including, without limitation, to all decisions regarding editing, lighting, filming, timing of publication, if any, length, quality, content and the like.

12.   **Indemnification.** The Author agrees to indemnify JoVE and/or its successors and assigns from and against any and all claims, costs, and expenses, including attorney's fees, arising out of any breach of any warranty or other representations contained herein. The Author further agrees to indemnify and hold harmless JoVE from and against any and all claims, costs, and expenses, including attorney's fees, resulting from the breach by the Author of any representation or warranty contained herein or from allegations or instances of violation of intellectual property rights, damage to the Author's or the Author's institution's facilities, fraud, libel, defamation, research, equipment, experiments, property damage, personal injury, violations of institutional, laboratory, hospital, ethical, human and animal treatment, privacy or other rules, regulations, laws, procedures or guidelines, liabilities and other losses or damages related in any way to the submission of work to JoVE, making of videos by JoVE, or publication in JoVE or elsewhere by JoVE. The Author shall be responsible for, and shall hold JoVE harmless from, damages caused by lack of sterilization, lack of cleanliness or by contamination due to

the making of a video by JoVE its employees, agents or independent contractors. All sterilization, cleanliness or decontamination procedures shall be solely the responsibility of the Author and shall be undertaken at the Author's expense. All indemnifications provided herein shall include JoVE's attorney's fees and costs related to said losses or damages. Such indemnification and holding harmless shall include such losses or damages incurred by, or in connection with, acts or omissions of JoVE, its employees, agents or independent contractors.

13.   **Fees.** To cover the cost incurred for publication, JoVE must receive payment before production and publication the Materials. Payment is due in 21 days of invoice. Should the Materials not be published due to an editorial or production decision, these funds will be returned to the Author. Withdrawal by the Author of any submitted Materials after final peer review approval will result in a US$1,200 fee to cover pre-production expenses incurred by JoVE. If payment is not received by the completion of filming, production and publication of the Materials will be suspended until payment is received.

14.   **Transfer, Governing Law.** This Agreement may be assigned by JoVE and shall inure to the benefits of any of JoVE's successors and assignees. This Agreement shall be governed and construed by the internal laws of the Commonwealth of Massachusetts without giving effect to any conflict of law provision thereunder. This Agreement may be executed in counterparts, each of which shall be deemed an original, but all of which together shall be deemed to me one and the same agreement. A signed copy of this Agreement delivered by facsimile, e-mail or other means of electronic transmission shall be deemed to have the same legal effect as delivery of an original signed copy of this Agreement.

A signed copy of this document must be sent with all new submissions. Only one Agreement is required per submission.

CORRESPONDING AUTHOR

Name:

Corrado Cali

Department:
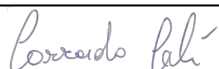
Biological and Environmental Sciences and Engineering

Institution:

KAUST (King Abdullah University of Science and Technology)

Title:

Research Scientist

Signature: *Corrado Cali*   Date: November 27th, 2018

Please submit a **signed** and **dated** copy of this license by one of the following three methods:
1.   Upload an electronic version on the JoVE submission site
2.   Fax the document to +1.866.381.2236
3.   Mail the document to JoVE / Attn: JoVE Editorial / 1 Alewife Center #200 / Cambridge, MA 02140

Thuwal, January 28th 2019

Dear Alisha:

many thanks for the constructive comments on the manuscript. As per her requests, we have attached a version of the manuscript with modifications highlighted as track-change to help follow each of the requests that have been raised.

We sincerely hope that all points have been addressed correctly and looking forward to the feedbacks from the editor.

With my best regards,

Corrado Calì,

On behalf of all authors.